*International Journal of Thermophysics, Vol. 11, No. 4, 1990*

# A Dynamic Technique for Measuring Surface Tension at High Temperatures in a Microgravity Environment[1]

**A. P. Miiller[2] and A. Cezairliyan[2]**

The feasibility of a dynamic technique for measuring surface tension of liquid metals at high temperatures in a microgravity environment is considered. The basic method involves heating a tubular specimen resistively from ambient temperature through its melting point in about 1 s by passing an electrical current pulse through it, while simultaneously recording the pertinent experimental quantities. Static equilibrium for the molten specimen may be achieved (at least for a short time) in a microgravity environment by splitting the current after it passes through the specimen tube and returning a fraction along the tube axis and the remaining fraction outside the specimen. Adjustments to the current split enable a balance between the magnetic and surface tension forces acting on the specimen. Values for surface tension are determined from measurements of the equilibrium dimensions of the molten specimen tube, and the magnitudes of the currents. Preliminary rapid melting experiments, performed during microgravity simulations with NASA's KC-135 aircraft, yield a value for the surface tension of copper at its melting point which is in reasonable agreement with literature data.

**KEY WORDS:** copper; dynamic technique; high temperature; liquid metals; melting point; microgravity; surface tension.

## 1. INTRODUCTION

The background and rationale for the development of millisecond-resolution dynamic techniques for use in a microgravity environment to study thermophysical properties of refractory liquid metals have been given in

[1] Paper presented at the First Workshop on Subsecond Thermophysics, June 20–21, 1988, Gaithersburg, Maryland, U.S.A.

[2] Thermophysics Division, National Institute of Standards and Technology (formerly National Bureau of Standards), Gaithersburg, Maryland 20899, U.S.A.



0195-928X/90/0700-0663$06.00/0 

another paper [1]. The present paper describes a feasibility study of a dynamic technique for measuring, under microgravity conditions, the surface tension of liquid metals at high temperatures.

The basic method consists of resistively heating a tubular specimen, mounted in a so-called "triaxial" configuration, from ambient temperature to temperatures above its melting point in about 1 s by passing an electrical current pulse through it and simultaneously measuring the radiance temperature of the specimen surface by means of a high-speed pyrometer [2], the electrical currents through and around the specimen, and recording the behavior of the specimen by means of a high-speed framing camera. In the triaxial configuration, static equilibrium for the molten specimen tube, which is mounted concentrically with respect to the current return paths, is achieved (at least for a short time) by suitable adjustments of the return currents. Values for surface tension are determined from measurements of the equilibrium dimensions of the molten specimen, and the magnitudes of the currents.

In the following sections, we first describe an analytical model of the triaxial configuration which enables surface tension to be expressed in terms of measurable experimental parameters. Rapid melting experiments, performed on copper specimen tubes during microgravity simulations with NASA's KC-135 aircraft, are then described. The results are analyzed in terms of the analytical model and the resultant value for surface tension of copper is compared with other literature data. Details regarding the construction and operation of the measurement system, designed for microgravity simulations with the KC-135 aircraft, have been given elsewhere [1].

## 2. ANALYTICAL MODEL OF THE TRIAXIAL CONFIGURATION

A schematic diagram of the "triaxial" configuration is given in Fig. 1. In this arrangement, the current $i$ through the specimen tube is split and returned along two paths: (1) a fraction $fi$ is returned along the axis of the specimen by means of a conducting rod, and (2) the remaining fraction $(1-f)i$ is returned outside the specimen by means of a concentric conducting tube.

Because of cylindrical symmetry, the magnetic field generated by the currents has only an azimuthal component $B_\theta$ which, in the interior of the specimen tube, is directed as shown with a magnitude proportional to $fi$ and, outside the specimen tube, is directed oppositely with a magnitude proportional to $(1-f)i$. Thus, the magnetic field will exert an outward pressure on the inside surface of the specimen tube, as well as an inward pressure on the outside surface, and so it may be possible to counter-

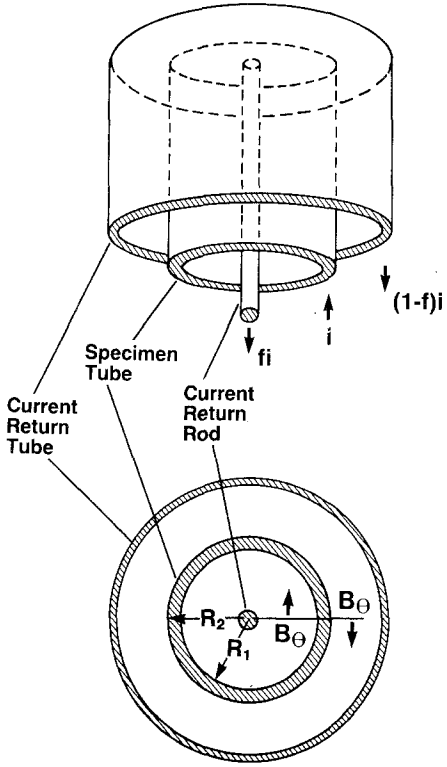


**Fig. 1.** Schematic diagram of a triaxial configuration for electrical current paths through and around a tubular specimen.

balance the inward pressure of surface tension on the melting specimen by a suitable adjustment in the return current split. This qualitative argument suggests that, under microgravity conditions, the triaxial configuration may provide the basis for a new technique to measure surface tension of liquid metals.

For a quantitative analysis, let us consider a specimen tube for which the length of the melt zone is approximately equal to or less than the tube diameter, as shown in Fig. 2 (the current return rod is not shown for clarity). Results of microgravity experiments (see Section 4) indicate that, when an imbalance between magnetic and surface tension forces exists at the onset of melting, the melt zone will expand (as shown in Fig. 2) or contract radially as required until geometrical stability is again reestablished (at least for a short time); in principle it is possible, although difficult, to select a current split which will achieve an exact initial balance so that the cylindrical geometry of the tube is maintained during melting.

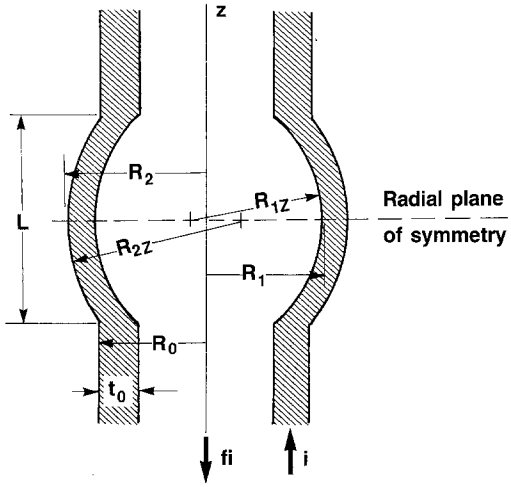


**Fig. 2.** Schematic representation of a tubular specimen with a finite melt zone mounted in a triaxial configuration (current return paths not shown).

In general, the motion of the liquid in the melt zone will follow the Navier–Stokes equation for an incompressible fluid:

$$\rho \frac{d\vec{v}}{dt} = \rho\vec{g} + \vec{j} \times \vec{B} - \vec{\nabla} p + u^* \nabla^2 \vec{v} \tag{1}$$

where $\rho$ and $u^*$ are the density and viscosity of the liquid, $\vec{g}$ is the gravitational acceleration, $\vec{j}$ is the current density, $\vec{B}$ is the magnetic flux density, and $p$ is the pressure in a unit volume moving with velocity $\vec{v}$. Under microgravity conditions ($\vec{g} \approx 0$) the required force balance for static equilibrium ($\vec{v} = 0$) in the melt zone is determined by Eq. (1), which simplifies to

$$\vec{\nabla} p = \vec{j} \times \vec{B} \tag{2}$$

In the radial plane of symmetry through the center of the melt zone, the pressure difference required to balance the net magnetic force may be determined from Eq. (2) by integration:

$$\int_{p_1}^{p_2} dp = -\int_{R_1}^{R_2} jB_\theta(r)\, dr \tag{3}$$

where $p_1$ and $p_2$ are the pressures at the inner and outer surfaces of the melt zone at its midpoint, $R_1$ and $R_2$ are the respective equilibrium radii,

and $B_\theta(r)$ is the magnitude of the azimuthally directed magnetic field. The pressures may be expressed in terms of the surface tension $\gamma$ as follows:

$$p_1 = -\gamma(1/R_1 + 1/R_{1z}) + P_c \tag{4}$$

$$p_2 = \gamma(1/R_2 + 1/R_{2z}) + P \tag{5}$$

where $R_{1z}$ and $R_{2z}$ are the axial radii of curvature of the inner and outer surfaces, and $P_c$ and $P$ are the pressures exerted by the gas environment at the respective surfaces. The magnetic field within the specimen ($R_2 \leqslant r \leqslant R_1$), in the radial symmetry plane, may be determined from Ampere's law:

$$B_\theta(r) = \frac{\mu_0 j}{2r}[r^2 - R_1^2 - f(R_2^2 - R_1^2)] \tag{6}$$

where the specimen tube and current return rod are assumed to be ideally nonmagnetic, that is, their magnetic permeability is given by $\mu_0 = 4\pi \times 10^{-7}\,\mathrm{H \cdot m^{-1}}$.

Evaluating the integrals and solving for $\gamma$ in terms of the current $i$, one obtains the following expression for the case of equal gas pressures ($P_c = P$):

$$\gamma = \frac{\mu_0 i^2 R}{2\pi^2(R_2^2 - R_1^2)}\left[\left(\frac{R_1^2}{R_2^2 - R_1^2} + f\right)\ln(R_2/R_1) - \frac{1}{2}\right] \tag{7}$$

where the parameter

$$R = [1/R_2 + 1/R_1 + 1/R_{2z} + 1/R_{1z}]^{-1} \tag{8}$$

The principal radii of curvature of the inside surface ($R_1$ and $R_{1z}$) cannot be observed directly and, so, must be inferred from measurable quantities.

Conservation of volume (as required by incompressibility of the liquid) may be satisfied by assuming that the cross-sectional area of the tube (in the radial plane) is constant during radial expansion (or contraction) of the melt zone, and therefore,

$$R_1 = [R_2^2 - t_0(2R_0 - t_0)]^{1/2} \tag{9}$$

where $t_0$ and $R_0$ are the wall thickness and outer surface radius of the tube at the onset of melting.

In the case of a "short" melt zone (length $L \lesssim 2R_0$) which undergoes a small radial expansion or contraction ($R_2 \sim R_0$) to achieve static equilibrium, the axial curvature of each surface may be approximated by

circular arcs spanning the full length of the melt zone. Simple geometrical considerations then yield

$$R_{2z} = \frac{(R_2 - R_0)^2 + (L/2)^2}{2(R_2 - R_0)} \tag{10}$$

and

$$R_{1z} = \frac{(R_1 - R_0 + t_0)^2 + (L/2)^2}{2(R_1 - R_0 + t_0)} \tag{11}$$

Therefore, Eqs. (7)–(11) express the surface tension of the specimen in terms of six experimentally observable quantities: the current $i$ through the specimen, the fraction $f$ of current returned along the tube axis, the wall thickness $t_0$ and radius $R_0$ of the tube just before melting, and the equilibrium radius $R_2$ and length $L$ of the melt zone.

## 3. MEASUREMENTS

In order to test the validity of the analytical model, we selected copper as the candidate specimen material, primarily for two reasons: (1) considerable data on surface tension of copper already exist in the literature, and (2) the melting point of copper is sufficiently high to permit the use of high-speed pyrometry.

The specimens, which were fabricated from 99.99% pure copper tube stock, had the following nominal dimensions: thickness, 0.1 mm; diameter, 6 mm; and length between electrodes, 25 mm. Each specimen was mechanically treated to remove surface oxides and then stored in an argon environment prior to mounting in an experiment chamber for the KC-135 flight experiments.

The present work required the design and construction of a new experiment chamber which utilized the triaxial configuration. A schematic diagram of the experiment chamber is illustrated in Fig. 3. The tubular specimen is clamped between a stationary lower electrode and an upper electrode which is attached to two flexible (phosphor-bronze) bellows to allow for thermal expansion of the solid specimen in the axial direction; the specimen is mounted under a small tension at room temperature in order to approximate the desired condition of zero axial stress during melting. The upper bellows is clamped to a copper rod which enables a fraction of the current to be returned along the axis of the specimen. The lower bellows is soldered to a concentric brass tube which permits the remaining fraction of current to be returned outside of the specimen; axial slots in the brass tube enable the specimen to be viewed by the high-speed pyrometer

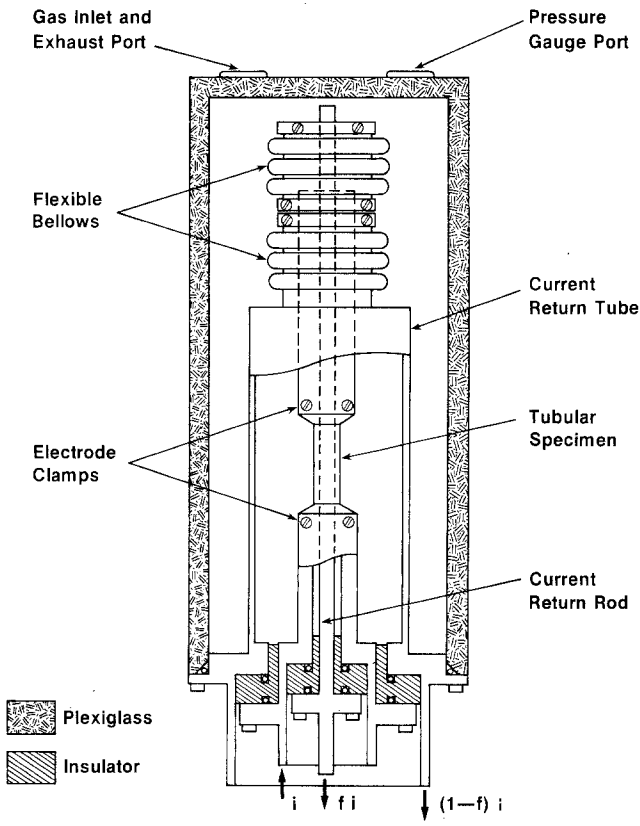


**Fig. 3.** Schematic diagram of an experiment chamber which utilizes a triaxial configuration for studying the stability of tubular specimens during rapid melting in a microgravity environment.

and framing camera. The current split is controlled by means of an adjustable resistor (thin-walled Inconel tube) in one of the two current return paths in the pulse-heating system. A removable plexiglass cylindrical cover provides access for mounting the specimen and enables melting experiments to be performed with the specimen in an argon environment at nominal pressures ($\sim$0.2 MPa). A total of eight chambers was constructed to enable the performance of a series of melting experiments during each KC-135 flight.

During a given flight, the aircraft was flown through a series of parabolic maneuvers, each yielding a period of simulated low gravity of about 20 s. In a typical experiment, the specimen was rapidly heated during the low-$g$ period from ambient temperature through its melting point by

passing an electrical current pulse through it. Depending on the experiment, the duration of the heating period varied between about 0.5 and 2 s. During heating, the behavior of the specimen was photographed by the framing camera operating at 1000 frames per second, while signals from the high-speed pyrometer, the $z$-axis accelerometer, and the current measuring devices were recorded every 2 ms by the digital data acquisition system.

The magnitude of the current pulse used to melt the specimen ranged from approximately 700 to 1100 A, yielding heating rates in the range 500 to 2000 $K \cdot s^{-1}$. The average minimum $g$ level during melting was typically about $1 \times 10^{-2} g$, with a standard deviation of approximately $2 \times 10^{-2} g$; deviations from the average were due to vibrations transmitted to the specimen mount from the aircraft and from the framing camera. Improved vibration isolation in the present work resulted in a threefold reduction of vibrational "noise" when compared with earlier microgravity experiments [1].

## 4. RESULTS

Figure 4 presents sequences of photographs taken by the high-speed framing camera during three microgravity-simulation experiments in which the current split fraction $f$ was 0.67, 0.78, and 0.84, respectively. The times shown to the left of the photographs refer to the elapsed time during melting; the melting period was readily identified by a plateau in the temperature-time data recorded on the high-speed photographs (not shown here; see discussion in Ref. 1). In order to identify the melt zone, the specimen was illuminated by an external light source, aimed at an angle with respect to the camera line of sight. As a result, light from the external source was diffusely scattered into the camera lens by the "rough" solid surface of the specimen, yielding a bright axial line in each photograph, but was specularly reflected out of the field of view by the smooth molten surface. Therefore, the absence of a bright axial line identifies the melt zone of the specimen. In the present work, the melt zone length $L \lesssim 2R_0$.

In the experiment where $f = 0.78$, the specimen retained its cylindrical geometry through the entire melting period of 60 ms, during which the melt zone appeared to be in static equilibrium. The situation is less clear in the other experiments, in which the melt zone either contracted ($f = 0.67$) or expanded ($f = 0.84$) during melting. In order to determine the midpoint radius of the melt zone as a function of time, a rear-projection digitizer/computer system was used to analyze the high-speed photographs (frame by frame) for each microgravity experiment.

The results for an experiment with $f = 0.84$ are presented in Fig. 5, where the midpoint radius $R_2$ is plotted in units of $R_0$ (the tube outer

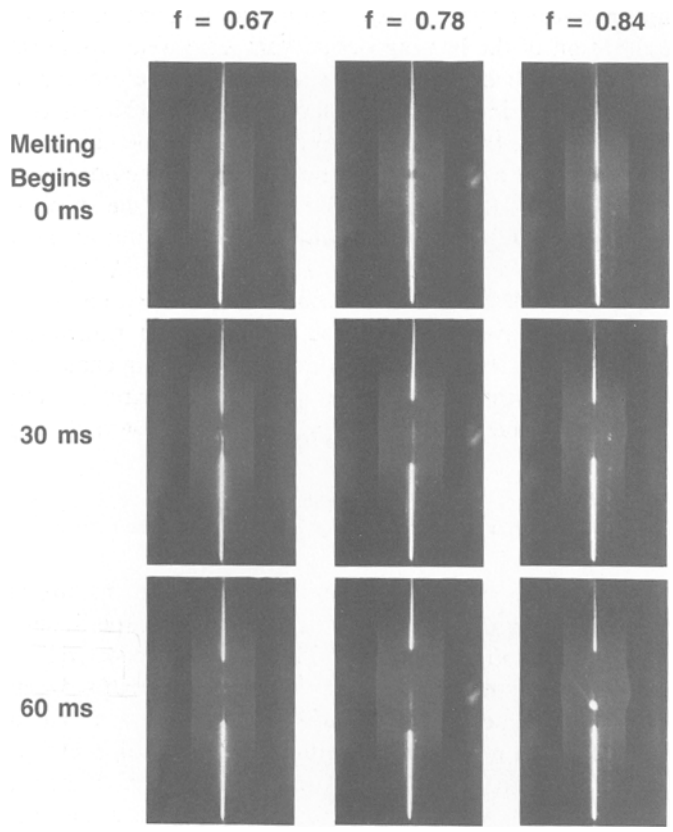


**Fig. 4.** Sequences of photographs of tubular copper specimens taken during three rapid-melting experiments in a microgravity environment, each with a different value of $f$ (fraction of current returned along the tube axis).

radius just before melting) as a function of elapsed time during melting. It may be seen that, after an initial period, the specimen softens and the radius increases to an equilibrium value, $R_{2E}$; the subsequent rapid increase in radius is due to a premature rupturing of the thin-walled tube (see discussion below). The important result illustrated here is that, even in cases where the melt zone expands (or contracts) during melting, static equilibrium may be achieved for at least a short time.

The equilibrium values, $R_{2E}$, observed in eight microgravity experiments, and the corresponding values of $L$, $i$, $f$ (in the range 0.77 to 1.0), $R_0$, and $t_0$ were used in Eqs. (7)–(11) to determine the surface tension of copper at its melting point; the results are given in Fig. 6 as a function of

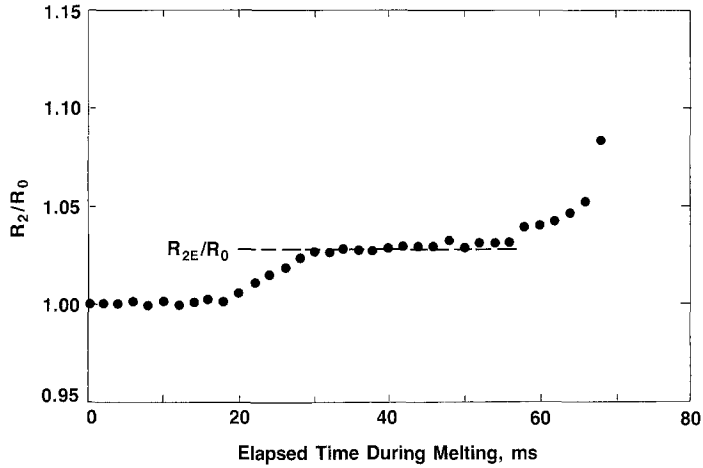


**Fig. 5.** Variation of the midpoint radius $R_2$ of a melt zone during rapid melting in a microgravity environment; $R_0$ is the radius of the tubular specimen just before melting.

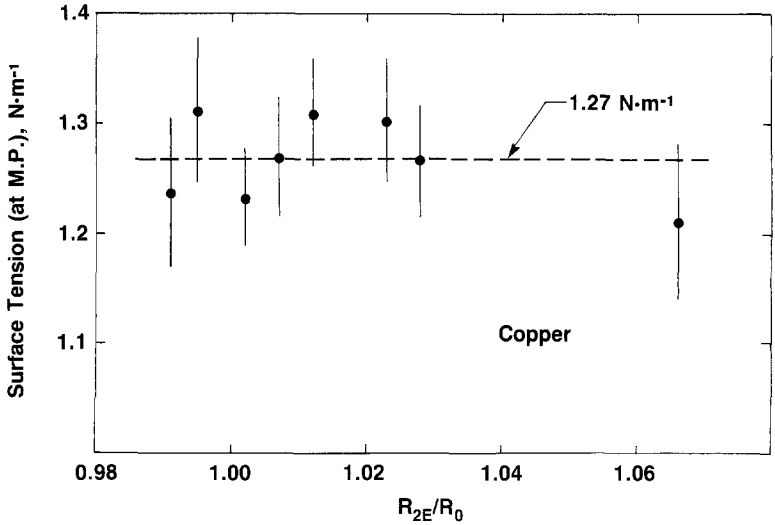


**Fig. 6.** Results for the surface tension of copper at its melting point as a function of the equilibrium value for $R_2$, i.e., $R_{2E}$, observed in eight microgravity experiments. The bars indicate the estimated uncertainties, which are due primarily to errors in determining the equilibrium radius $R_{2E}$ and melt zone length $L$ from the photographs.

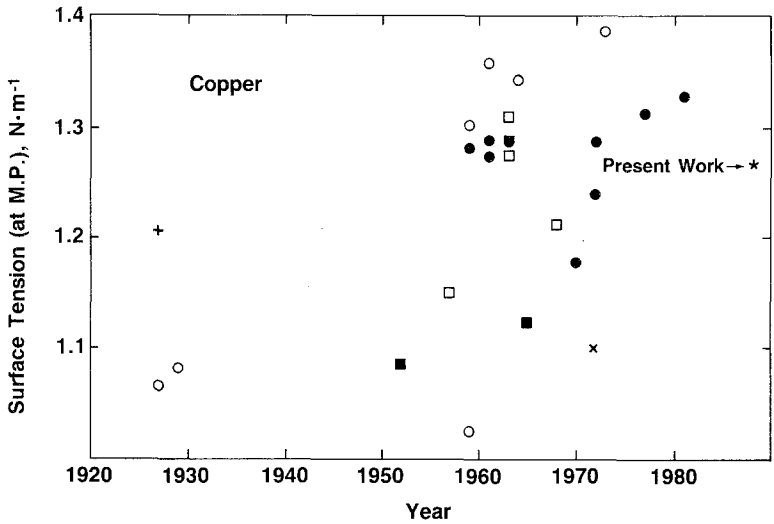


**Fig. 7.** Comparison of the present value for surface tension of copper at its melting point with other literature data [3, 4]. The various symbols refer to different measurement techniques, as follows: (+) capillary rise; (×) drop force; (□) drop mass; (■) pendant drop; (○) maximum bubble pressure; (●) sessile drop; (★) dynamic pulse heating.

$R_{2E}/R_0$. The estimated uncertainty in the resultant values for surface tension varied between about 4 and 6%, depending on the experiment, and was due primarily to the uncertainties in determining $R_2$ and $L$ from the high-speed photographs. The results for the surface tension of copper at its melting point were averaged, yielding a mean of $1.27\ \mathrm{N \cdot m^{-1}}$, with a standard deviation from the mean of $0.04\ \mathrm{N \cdot m^{-1}}$.

## 5. DISCUSSION

A comparison of the present result with a compilation [3] of earlier literature data, as well as more recent work [4], is given in Fig. 7. The large scatter in reported values reflects the difficulties involved in the measurement of surface tension at high temperatures. The various symbols refer to six different measurement techniques, other than the present dynamic technique. The filled circles refer to the sessile drop technique, which appears to have been the method of choice in recent years and seems to yield data with the least amount of scatter. As may be seen, the present value (asterisk) is in reasonably good agreement with these results, which suggests that the present dynamic technique is a feasible method for measuring surface tension of liquid metals, at least at their melting points.

As mentioned above, the thin-walled specimen tubes used in the

present experiments tended to rupture during melting, prior to any significant excursion into the liquid phase. This behavior may be the result of (a) microscopic fluctuations which, due to the thin wall (0.1 mm), could produce a small pinhole causing the tube to burst and/or (b) instabilities generated by perturbations of the specimen inner and outer surfaces. In the present work, no perturbations were observed in the outer surface prior to rupturing of the molten tube.

The effect of axisymmetric surface perturbations on the stability of an infinitely long current-carrying liquid tube in a triaxial configuration has been the subject of a recent theoretical investigation [5]. The results suggest that, for finite melt zones with $L \lesssim 2R_0$, the configuration may be stable as long as $f > 0.6$.

Additional microgravity experiments are being planned to investigate the effect of wall thickness and melt zone length on specimen stability. If the problem of molten tube rupture is resolved, significant temperature excursions into the liquid phase should be possible, which will enable the determination of other thermophysical properties, such as heat of fusion and surface tension, heat capacity, and electrical resistivity of the liquid specimen.

## ACKNOWLEDGMENTS

This work was supported by the Microgravity Science and Applications Division of NASA. The authors gratefully acknowledge the assistance of P. Giarratano of NBS/Boulder, R. Shurney of NASA/MSFC, and R. Williams of NASA/JSC during the preparations for and the performance of the microgravity experiments.

## REFERENCES

1. A. Cezairliyan and A. P. Miiller, *Int. J. Thermophys.* **11**:653 (1990).
2. A. Cezairliyan and G. M. Foley, in preparation.
3. D. A. Harrison, D. Yan, and S. Blairs, *J. Chem. Thermodyn.* **9**:1111 (1977).
4. B. Gallois and C. H. P. Lupis, *Metall. Trans. B* **12B**:549 (1981).
5. R. A. MacDonald *J. Appl. Phys.* **66**:5302 (1989).